

# Secure and secret cooperation of robotic swarms by using Merkle trees

Eduardo Castelló Ferrer\*<sup>1</sup>, Thomas Hardjono<sup>2</sup>, Alex ‘Sandy’ Pentland<sup>1,2</sup>

<sup>1</sup>MIT Media Lab, Massachusetts Institute of Technology, Cambridge, MA 02139, USA

<sup>2</sup>MIT Connection Science & Engineering, Massachusetts Institute of Technology, Cambridge, MA 02139, USA

Email: {ecstll, hardjono, pentland}@mit.edu

**Abstract**—Swarm robotics systems are envisioned to become an important component of both academic research and real-world applications. However, in order to reach widespread adoption, new models that ensure the secure cooperation of these systems need to be developed. This work proposes a novel model to encapsulate cooperative robotic missions in Merkle trees, one of the fundamental components of blockchain technology. With the proposed model, swarm operators can provide the “blueprint” of the swarm’s mission without disclosing raw data about the mission itself. In other words, data verification can be separated from data itself. We propose a system where swarm robots have to “prove” their integrity to their peers by exchanging cryptographic proofs. This work analyzes and tests the proposed approach for two different robotic missions: foraging (where robots modify the environment) and maze formation (where robots become part of the environment). In both missions, robots were able to cooperate and carry out sequential operations in the correct order without having explicit knowledge about the mission’s high-level goals or objectives. The performance, communication costs, and information diversity requirements for the proposed approach are analyzed. Finally, conclusions are drawn and future work directions are suggested.

**Keywords**—Distributed Robotics; Cooperative Robotics; Data Privacy; Blockchain; Research Challenges; Merkle Trees; Verifiable Robotics; Trustable Robotics; Reliable Robotics

## I. INTRODUCTION

Swarm robotics systems have the potential to revolutionize many industries, from targeted material delivery [1] to precision farming [2]. Boosted by technical breakthroughs, such as cloud computing [3], novel hardware design [4], and manufacturing techniques [5], swarms of robots are envisioned to play an important role in both industrial [6] and urban [7] activities. The emergence of robot swarms has been acknowledged as one of the ten robotics grand challenges for the next 5-10 years that will have significant socioeconomic impacts [8]. However, despite having such a promising future, many important aspects which need to be considered in realistic deployments are either underexplored or neglected [8].

One of the main reasons why swarms of robots have not been widely adopted in real-world applications is because there is no consensus on how to design swarm robotics systems that include perception, action, and communication among large groups of robots [8]. In addition, recent research points out that the lack of security standards in the field is also hindering the adoption of this technology in data-sensitive areas (e.g., military, surveillance, monitoring) [9]. These research gaps are motivating scientists to focus on new fields of study such as applied swarm security [10], [11] and privacy [12], [13] as well as to revisit already accepted assumptions in the field.

From the origins of swarm robotics research, robot swarms were assumed to be fault-tolerant by design, due to the large number of robot units involved [14]. However, it has been shown that a small number of partially failed robots (with defective sensors, broken actuators, noisy communications devices, etc.) can have a significant impact on the overall system reliability and performance [15]. The first surveys on swarm robotics security were presented in [16], [17]. These works identified physical capture and tampering with members as significant threats to robot swarms. Physical capture of a robot might not only lead to loss of availability but also to the capture of security credentials or critical details of the swarm operation [18]. For instance, if a robot is tampered with and reintroduced into the swarm, an attacker might influence the behaviour of the whole system [14] and eventually hinder the entire operation [19]. These attacks would be unique to swarm robotics technology and are particularly critical in situations where robot swarms must share data among individual robot units or with human operators.

		Awareness of others	
		Aware	Not-aware
Types of goals	Individual	Collaborative (3542)	
	Shared	Cooperative (7002)	Collective (1568)

Figure 1. Classification schema for the distributed systems field based on [20] (to which the swarm robotics field belongs). Types of goals (individual or shared) and degree of awareness of other members (aware or not aware) are the main factors to distinguish between collective, cooperative, and collaborative systems. In parentheses, the number of research documents published with the terms “collaborative robots”, “cooperative robots”, and “collective robots” respectively from 1972 to 2018<sup>2</sup>

A convenient way to approach the swarm robotics domain is by pointing out the types of synergies that can occur between the robots [20]. As illustrated in Fig. 1, we find it helpful to view these synergies along two different factors: 1) the types of goals robots have and 2) whether robots have awareness of others in the swarm. Regarding the types of goals, we distinguish two types of systems: individual or shared goals. In terms of the awareness-of-others factor, we classify the systems into two categories: aware and not aware. By aware in this situation, we refer to whether robots have the capability to reason about the behavior and future actions of their peers. For

Corresponding author: Eduardo Castelló Ferrer, ecstll@mit.edu

<sup>2</sup>Source: Scopus research database

instance, robots that are not aware may sense the proximity of local robots and move accordingly to maintain a certain distance and avoid collisions, but otherwise perform no other explicit exchange of information.

Perhaps the simplest type of interaction in Fig. 1 is the collective one. *Collective robotics* traditionally takes inspiration from social animals [21], [22], [23] and typically involve the use of a large number of robots in order to achieve shared goals (pattern formation [24], navigation [25], etc.). However, collective robotics platforms [26], [27] are still resource-limited systems where explicit communication and accurate reasoning about other robots' intentions remains a challenge. An illustrative example in this field is the use of stigmergy [28], [29], [30], a type of "in-field" (rather than explicit) communication that can be used to self-organize collective motion [31], construction [32], etc. In contrast, *Collaborative robotics* normally involves small to middle-sized highly specialized teams of robots with different abilities [33], [34]. Collaborative robots work together by exchanging large amounts of information and sharing sensory, actuation, or computation capabilities to help team members reach their individual goals [33], [35]. However, collaborative robotic missions normally require heterogeneous teams of robots [36], which might limit the applicability of these systems to ad-hoc or context-specific missions.

*Cooperative robotics* is based on the idea that multiple robots share common goals and are aware of the intentions of other robot peers. Examples of cooperative robotics include numerous robots working as a group and reasoning about each other's abilities to carry out a shared task, such as cooperative grasping and transportation of objects [37], [38], environmental monitoring [39], or extra-planetary exploration [40]. In cooperative robotics missions, robots may be working on different aspects of the higher-level task, therefore, they have to ensure that they are still working together to fulfill the common objectives. Traditionally, cooperative robotic missions are not limited by the communication and computation constraints of collective robotics platforms nor do they require heterogeneous teams of specialized robots to fulfill individual goals. Due to the lack of these limitations, the cooperative robotics field has turned into a popular area of research (Fig. 1) and therefore a good test bed for new models and methods in the distributed robotics space.

In previous work in the cooperative robotics field, researchers hard-coded the complete set of rules that trigger the transitions from task to task [32] in all robots within a mission. Even though this distributed approach is more robust and fault-tolerant than centralized methods, it significantly increases the attack surface for an attacker to figure out the swarm's high-level goals and modify the system's behavior [18]. Due to these concerns, in this work, we aim to shed light on the following questions: How can we make sure that robotic swarms can cooperate while minimizing security risks such as physical capture or tampered members? Is there a way to provide the "blueprint" of a robotic mission without describing the mission itself? In other words, is it possible that robot swarms fulfill step-by-step (i.e., sequential) missions without having explicit knowledge about the mission's objectives? To answer these questions, we propose a model which allows robots to cooperate without exposing the high-level information about the swarm's goals. In this paper, we explore for the first time the

idea of encapsulating robotic missions into Merkle trees. More specifically, we introduce a framework where data verification is separated from data itself. By exchanging cryptographic "proofs" within the swarm, robots are able to "prove" to their peers they know specific pieces of information included in the swarm's high-level mission and therefore cooperate towards its completion.

The remainder of this paper is structured as follows. Section II summarizes related work on Merkle trees and their applications outside the robotics field. Section II-A provides a formalization of Merkle trees and introduces the concept of "proof". Section III describes the setup of our experiments including the type of mission, robots, simulator and analysis metrics used to evaluate the proposed approach. Section IV presents the results of our experiments. Section V discusses the results obtained and proposes future directions where our approach also shows promising results. Finally, Section VI provides our conclusions.

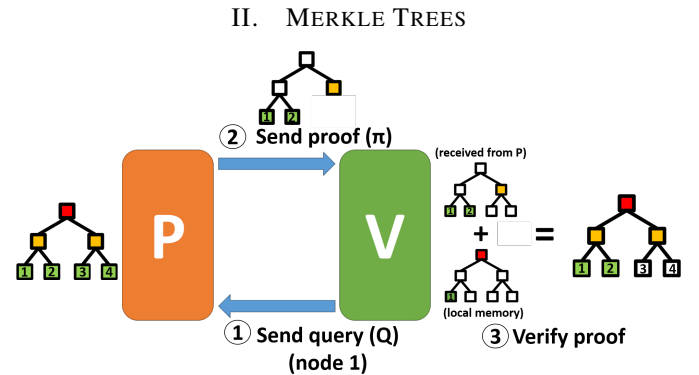
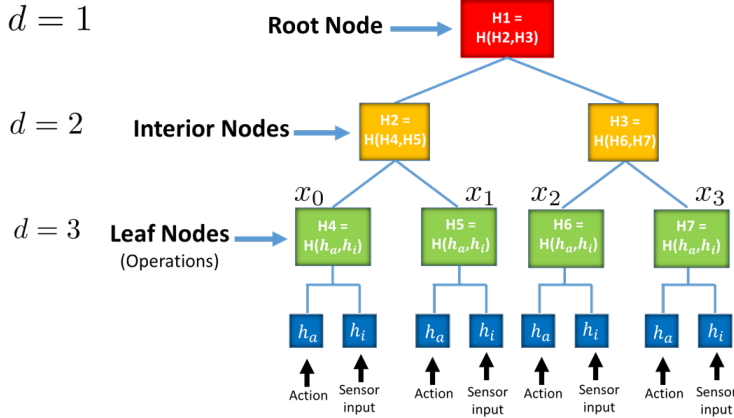


Figure 2. Workflow between *provers* (P) and *verifiers* (V). (1) V sends a query (Q) to P regarding a particular node (e.g., node 1). (2) P sends a proof (chain of hashes) ( $\pi$ ) that demonstrates knowledge about the requested node. (3) V verifies the proof by computing in a bottom-up fashion the received information. The proof is regarded as valid if V can generate the root node it kept in memory by using  $\pi$ .

A Merkle Tree (MT) [41] is a hash-based tree structure where data is not stored in the interior nodes but in the leaves. MTs belong to the family of Authenticated Data Structures (ADS), a type of data objects whose operations can be carried out by an untrusted third party. Two main roles: *provers* (P) and *verifiers* (V) are involved when using MTs. Provers store the data of interest encapsulated in an MT and are able to answer queries about it. Verifiers send queries to provers and in exchange they receive a "proof". A proof is a piece of information by which one party (P) can demonstrate to another party (V) that they know a value, without conveying any information apart from the fact that they know that specific value. Verifiers can check whether any piece of information belongs to the MT by checking the validity of the proof received. Fig. 2 shows a general description of this process. MTs have two main properties: correctness and security. On the one hand, correctness implies that a proof can be easily generated to verify and demonstrate that a piece of information is known and correct. This can be done without exposing the raw information itself by using cryptographic hashes. On the other hand, security implies that a computationally bounded, malicious agent cannot forge an incorrect result and therefore

(a)



(b)

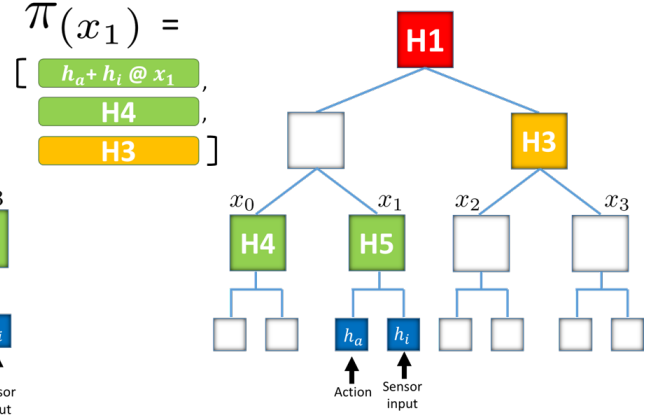


Figure 3. (a) Merkle Tree (MT) implementation ( $d = 3$ ) with 4 leafs, 2 interior, and 1 root nodes. Each leaf node (green) encapsulates the hash of two hashes: a robot action ( $h_a$ ) and a robot sensor input ( $h_i$ ). Each leaf node represents one atomic operation robots should complete sequentially ( $x_0, x_1, \dots, x_n$ ) in order to fulfill the swarm’s mission. Interior nodes encapsulate the hash of their two children, the same way that the root node encapsulates the hashes of its two interior nodes. (b) Describes the path (in color) in order to get the proof for leaf node  $x_1$ .

only agents that know the appropriate information can generate valid proofs.

In previous literature, MTs have been used for a wide variety of applications ranging from efficient data authentication [42], sharing [43] and integrity [44] to validation in large datasets, sensor networks [45], [46], software updates [47], etc. However, to the best of our knowledge, no research work has focused on the use of MTs in the field of robotics. In this work, we propose a model by which high-level missions can be encapsulated within an MT as a set of atomic operations performed by a swarm of robots. By searching the environment, robots are able to obtain sensor information and check whether potential actions are included in the MT (or not). In the affirmative case, robots are able to prove to their peers that certain parts of the mission were discovered, carried out, and completed by using MT proofs.

#### A. Merkle tree proofs

An MT of depth  $d$  represents a tree of  $n = 2^{d-1}$  leaf nodes:  $x_0, \dots, x_{n-1}$ . Each leaf node encapsulates a hash string of an associated operation, while each interior node contains the hash of the combination of its two children. A depiction of a complete MT for  $d = 3$  is given in Fig. 3 (a). Each leaf node (green blocks) encapsulates the combined hash of two hashes:  $h_i$  (sensor’s input) and  $h_a$  (robot’s action). These two hashes describe an atomic operation within the swarm’s high-level mission. For instance, the hash of the action “carry to target” ( $h_a$ ) and the hash of the sensor input “red token” ( $h_i$ ) would be included in one of the leaf nodes by using the hashing function  $H$ :  $H_{x_i} = H(h_a, h_i)$ . As outlined in Fig. 2, when  $V$  queries  $P$  it retrieves the value  $x_i$  at index  $i \in [0, n - 1]$ . Then,  $P$  returns the value  $x_i$  together with a chain of digests  $\pi$  needed to compute the root node digest (red block).  $V$  keeps (at least) a copy of the root node hash itself, and checks  $\pi$  by trying to recompute the root node hash in a bottom-up manner.

Fig. 3 (b) shows the proof  $\pi$  for a fetch at the leaf position  $x_1$ . It consists of four elements in sequence, the two hashes  $h_a$

and  $h_i$ , the hash H4, and the hash H3. Then, the verification proceeds bottom up:  $V$  computes the hashes of the two hashes  $h_i$  and  $h_a$ , which is H5, and concatenates it with the hash of H4 provided in  $\pi$ . Next, it concatenates H4 and H5 and computes the hash of what should be the digest for node H2. Then, it concatenates H3 provided in  $\pi$ , with its computed digest from the previous process, and hashes the result. Finally, it confirms whether this computed digest equals H1 (root node hash).

As mentioned before, we are interested in MT’s correctness and security. First, correctness implies that when  $P$  executes a query  $Q$  over its own MT, then  $V$  gets the same outcome as it would have if it had just computed  $Q$  locally. This property opens the path towards secret cooperation between agents since encrypted verification data can be exchanged within the swarm without disclosing any “raw” or “unprotected” information. Second, security implies that a computationally limited, deceiving  $P'$  cannot induce  $V$  to admit a faulty answer. The basis of this property is the use of collision-resistant hashes: if  $P'$  can cause  $V$  to accept an incorrect answer then the proof returned by  $P'$  will yield a collision (i.e., two different inputs produce the same output hash value). This research assumes the hash generation method used (SHA3-256) is collision-free, since (in theory) the probability that different inputs produce the same output is negligible. This property leads the way towards secure cooperation between agents.

### III. EXPERIMENTAL SETUP

Fig. 4 shows the initialization process of our experiments. For a start, we assume that an external entity (e.g., the swarm’s operator) designed and pre-computed a valid MT where all operations to fulfill the swarm’s mission are included in the correct order (1). Then, the resultant MT is broadcast to all the robots (2) before the mission starts (3). During the mission, robots can check whether the combined hash of potential actions ( $h_a$ ) upon specific sensor’s inputs ( $h_i$ ) can be related to their MT copy by trying to generate a valid proof. In this

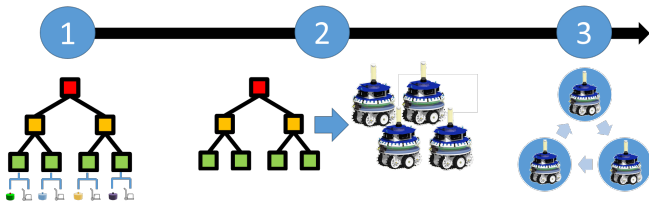


Figure 4. Experiment’s initialization process. (1) The swarm’s operator generates a valid MT where all operations to fulfill the swarm’s mission are included in the correct order. (2) The MT is broadcast to all swarm robots. (3) The experiment starts.

work, we tackle the case in which  $m$  operations must be performed in a specific order (i.e., sequentially) and without repetitions. As described in [48], our problem scenario can be understood as SO-SR-IA. In Single Operation (SO), robots are only able to execute one operation at a time. In Single Robot (SR), operations requires exactly one robot to achieve them. Finally, Instantaneous Assignment (IA) means that the available information concerning the robots, the operations, and the environment permits only an instantaneous allocation of operations to robots, with no planning for future allocations. The mission is finished once all operations are fulfilled in the right order and the MT is regarded as completed.

#### A. Foraging mission

Now, we introduce a robot foraging mission where each operation implies searching, retrieving, and transporting tokens to a central target location in the arena. The order in which these tokens have to be delivered is unknown by the robots during run time. The foraging mission is regarded as finished when at least one robot (i.e., the carrier of the last token) completes its MT.

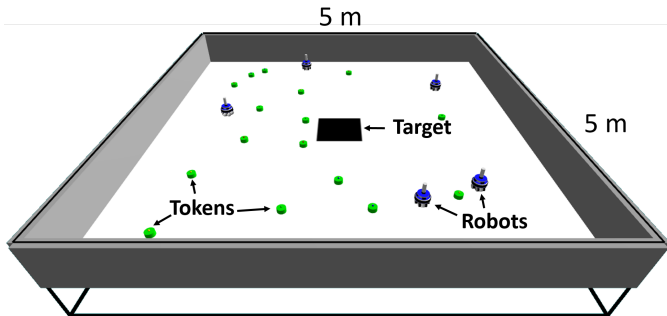


Figure 5. Simulation arena used in the foraging mission. The scenario was designed as a rectangular area of  $5 \times 5 m^2$  to provide adequate space for a small swarm of robots. In the figure, robots, tokens, and a target location are placed together in the same space.

Fig. 5 is a snapshot of the simulation arena where the foraging experiments were conducted. The environment was designed as a rectangular area ( $5 \times 5 m^2$ ) with a central black square ( $0.5 \times 0.5 m^2$ ) representing the target location where footbot robots [49] (Fig. 6 (a)) need to transport the correct sequence of discovered tokens. Fig. 6 (b) depicts one of the solid green cylinders that is used as a token within the experiments. These tokens are 5 cm tall and 10 cm in diameter and have a colored LED marker at the top. Different color tokens represent different sensor inputs. In this work, we have limited the color palette to the following colors: green, red, blue, yellow, magenta, cyan, white, and orange. A

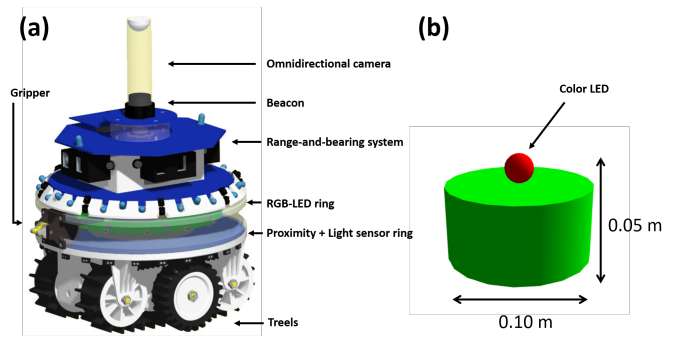


Figure 6. (a) Diagram of the simulated footbot together with its sensor layout. Footbot’s size and features correlate with real-world models for swarm and multi-agent systems. (b) Token used in the experiments. Tokens simulate 3D printed cylinders with the following dimensions: 5 cm tall and 10 cm in diameter. The colored sphere at the top of the token represents an LED marker to visually track and identify the tokens.

certain number of tokens of each color ( $D_{(i)}$ ) were randomly positioned at the beginning of each simulation run. All the experiments were conducted in ARGoS [50], a modular multi-robot simulator and development environment.

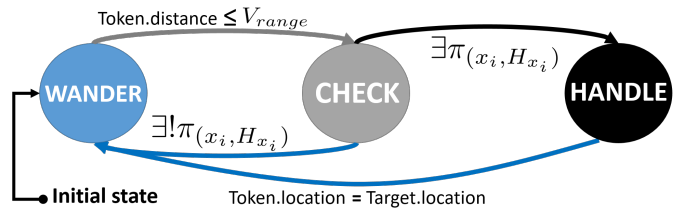


Figure 7. Finite State Machine for the robot behavior. Three main behaviors are coded in every robot. Robots in **Wander** mode search the environment looking for tokens. Once a token is found robots execute the **Check** behavior. Then, robots extract the information from the token (i.e., color) and generate both  $h_i$  and  $h_a$ .  $H_{x_i}$  is calculated from rehashing  $h_i$  and  $h_a$ :  $H_{x_i} = H(h_i, h_a)$ .  $H_{x_i}$  is verified against the current working leaf node ( $x_i$ ) of the robot’s MT. In case it is possible to generate a valid proof with the token’s information ( $\exists \pi(x_i, H_{x_i})$ ) the robot executes the **Handle** behavior: this makes the robot grab the token and place it in the target location (arena center). If not, the robot returns to the **Wander** mode.

Fig. 7 depicts the robot’s controller (FSM) for the foraging mission, which relies on three basic behaviors:

**Wander.** The robot performs a random walk searching for tokens. If the robot detects a token within its vision range ( $\text{Token.distance} \leq V_{range}$ ), it executes the **Check** behavior; otherwise it continues searching. During the execution of this action the robot is able to detect obstacles such as walls or other robots (within distance  $O_{range}$ ) and avoid them.

**Check.** Once a token is within the robot’s vision range, the robot can extract sensor information (point cloud data, RFID data, etc.) from it. In this stage, robots perceive the color of the LED marker associated with each of the tokens as a sensor input. This information is used by the robots in order to generate the sensor input hash ( $h_i$ ). The action hash ( $h_a$ ) encodes each of the possible actions (carry, push, stop, etc.) that robots can perform. For the foraging task,  $h_a$  is fixed to “carry to target”. Robots running the **Check** mode combine  $h_a$  and  $h_i$  to generate a meta-hash ( $H_{x_i} = H(h_c, h_a)$ ) that is used to generate the proof  $\pi$ . In case a proof  $\pi$  exists for the current working leaf node ( $x_i$ ):  $\exists \pi(x_i, H_{x_i})$ , the combination of

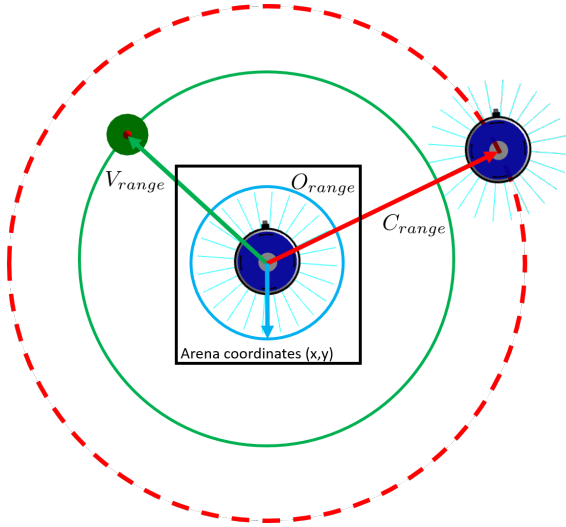


Figure 8. Robot communication and interaction diagram. Every robot controller relies on three main thresholds:  $O_{range}$  represents the range where obstacles are detected by robots in order to avoid collisions.  $V_{range}$  represents the robot's maximum vision range to detect tokens.  $C_{range}$  represents the minimum required distance for robots to communicate with one another. In addition, robots are able to locate themselves with global coordinates in the arena. This information helps them to find the target location (arena's center).

token color and action (i.e., operation) can be verified as part of the MT. Otherwise ( $\exists! \pi(x_i, H_{x_i})$ ), the robot returns to the **Wander** mode.

**Handle.** In case the robot generates a valid proof for the visible token, the robot approaches the token until it reaches a grabbing distance. In that moment, the robot activates its gripper (Fig. 6 (a)), grabs the token, and transports it to the center of the arena. Once the robot reaches its destination (Token.location = Target.location), the robot releases the token and changes the status of the  $x_i$  node as completed in its local MT. Finally, the robot increments the pointer of the current working leaf node:  $x_i = x_i + 1$  for  $x_i \in (0 \leq x_i \leq n - 1)$ .

Fig. 8, shows the robot interaction space. It is important to note that during the execution of the three behaviors explained previously, robots can exchange information with their peers (e.g.,  $x_i, \pi$ ). If robots are within a  $C_{range}$  distance from other robots, these can compare their MT copies by sending queries (Q) about their correspondent working leaf nodes ( $x_i$ ) and receive proofs ( $\pi$ ) in exchange as depicted in Fig. 2. By using this method robots can update, synchronize, and complete their own MT copies and therefore cooperate towards the fulfillment of the swarm's mission.

### B. Maze formation mission

In order to test our approach in a complementary scenario, we designed a new mission where instead of having the robots modify the environment (e.g., transport tokens), we decided to make them part of the environment (e.g., build a maze).

Fig. 9 (a) represents the "blueprint" of a  $5 \times 5$  maze where: 0 represents an empty space, 1 a wall, and \* and @ the entrance and the exit of the maze, respectively. As outlined in Fig. 4, we generated (during design time) a complete MT where leaf nodes (i.e., operations) encapsulate maze coordinates (instead of token colors). Following their FSM controller (Fig. 7), robots start exploring the arena in the **Wander** mode. Robots

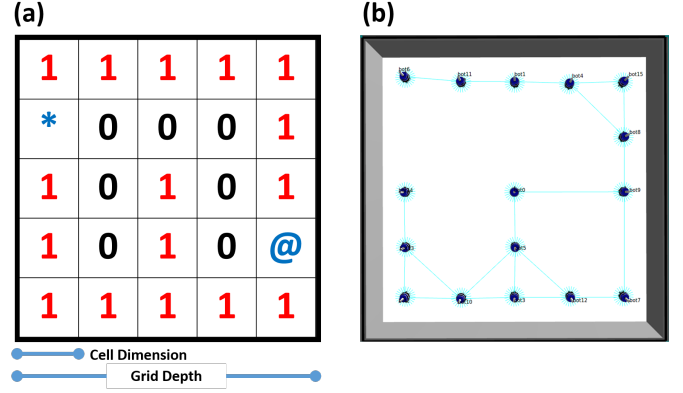


Figure 9. (a)  $5 \times 5$  matrix used in order to represent a maze. Four different elements are included in the array: 0 (black) represents an empty space, 1 (red) represents a wall, \* and @ (blue) represent the entrance and the exit of the maze, respectively. (b) The maze depicted in (a) built by a swarm of robots using the approach presented in this paper.

are able to locate themselves (Fig. 8) in the 2D arena ( $5 \times 5 m^2$ ). By knowing the cell dimensions ( $1 \times 1 m^2$ ) they can calculate the (x,y) coordinates of the grid depicted in Fig. 9 (a). Every time robots enter a new cell they execute the **Check** mode. Then, robots use the current grid (x,y) components as  $h_i$  and the hash of the action "stop" as  $h_a$ . In case robots generate a valid proof  $\pi$ , robots execute the **Handle** behavior, which leads them to find the center of the cell and stop there (Fig. 9 (b)). In contrast to the foraging example, the maze formation mission is finished once all operations have been completed as well as all robots have completed their correspondent MTs.

### C. Analysis Metrics

In order to evaluate and analyze the proposed approach we rely on three main metrics:

**Performance:** these measures convey how fast and reliably a particular mission is carried out. In this paper, we introduce the mission's finishing time ( $F_t$ ) as the metric that describes the amount of time required to fulfill the swarm's mission. In addition, we introduce the probability of success ( $P_s$ ) as an estimate that represents the probability that the system attains its target objective in an amount of time  $\tau$  [51]. Formally, let  $j \in \{1, \dots, k\}$  be the index of an experiment,  $r_j$  be the run-time of experiment j, and  $k^t \leq k$  be the number of successful experiments, that is, those experiments that fulfill:  $r_j < TC$  (Time Cap).  $P_s$  is defined as  $P_s(\tau \leq t) = \{j \mid r_j \leq t\} / k$  where,  $P_s(\tau \leq t)$  is an estimate of the probability of success of the system over time (up to TC).

**Communication Cost:** exchange of information is a crucial capability to make robots cooperate. Traditionally, swarm communication is constrained due to several factors: resource-limited robots, high-communication bandwidth requirements (e.g., when the swarm size increases), etc. For these reasons, we introduce the Communication Cost (CC) metric. CC represents the number of times the P-V workflow (Fig. 2) took place during the mission multiplied by the size (in bytes) of the proof ( $\pi$ ) robots exchanged. In case the MT is perfectly balanced ( $n = 2^{d-1}$ ), the size of the proof  $\pi$  is always  $\log_2(n) + 2$ : the number of hashes to reach the root node together with the  $h_i, h_a$  hashes. In missions where all robots need to complete their

correspondent MTs such as the maze formation one, CC can be accurately calculated with the following equation:

$$CC = P_n \cdot P_l \cdot |H| \quad (1)$$

where  $P_n = (R_n - 1 \cdot n)$  is the total number of proofs exchanged,  $P_l = \log_2(n) + 2$  is the length of the proof, and  $|H|$  is the size (in bytes) of the hash function used. The hash algorithm used in this work (SHA3-256) has a hash size ( $|H|$ ) of 32 bytes.

**Information Diversity:** in this research, robots are only in contact with the raw sensor and action information from the operations they carry out themselves. However, in cooperative robotics, robots are not typically limited to do only one operation per mission. Under this premise, individual robots might be able to accumulate raw or unprotected information and therefore be subject to attacks (e.g., physical capture). In response to this, we introduce a measure of “evenness” as a projection of how widely spread raw information might be within the swarm. The Shannon’s index (I) (i.e., Shannon’s entropy [52]) is a mathematical measurement used to characterize diversity:

$$I = - \sum_{i=1}^S p_i \ln p_i \quad (2)$$

where  $S$  is the total number of operations in the mission ( $n$ ) and  $p_i$  is the proportion of  $S$  made up of the  $i^{th}$  operation. Finally, Shannon’s equitability ( $I_e$ ) can be calculated by dividing  $I$  by  $I_{max}$ :

$$I_e = \frac{I}{I_{max}} \quad (3)$$

where  $I_{max} = \ln S$ .  $I_e$  assumes a value between 0 and 1 with 1 being complete “evenness”: all robots carried out the same number of operations and therefore were exposed to the same amount of raw information.

#### IV. RESULTS

A set of 50 simulation experiments were carried out to analyze the proposed approach in the foraging scenario shown in Fig. 5. MTs with different  $n$  values were used in order to increase the complexity and duration of the swarm’s foraging mission. In addition, the following parameters were used:  $D_{(i)} = 4$ , which implies that in simulations where the MT has 4 leaf nodes ( $n = 4$ ), a total of 16 tokens are present at the beginning of the simulations. From 1 to 5 robots ( $R_n$ ) were included at the beginning of the simulations. The robot communication range ( $C_{range}$ ) was initialized to 2 meters, the vision sensing distance ( $V_{range}$ ) was fixed to 0.50 meters, and finally the robot obstacle detection range ( $O_{range}$ ) was initialized to 0.10 meters. The Time Cap (TC) for each experiment was set to 10000 seconds.

Fig. 10 shows the finishing times ( $F_t$ ) and standard deviations for several MT length configurations ( $n$ ) and robot swarm sizes ( $R_n$ ). According to Fig. 10, the addition of more robots decreases the  $F_t$  of the foraging mission regardless of the length of the MT. However, these results suggest that once a certain number of robots is present ( $R_n \geq 3$ ), the length of the MT has a small impact on the  $F_t$  of the system.

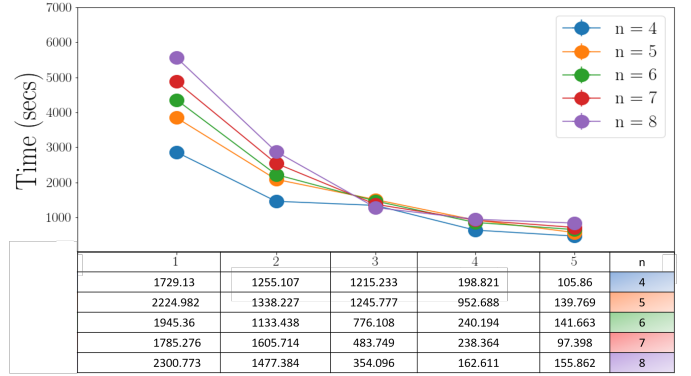


Figure 10. Average  $F_t$  (in secs) and standard deviations (in table format) for different MT lengths ( $n$ ) and robot swarm sizes ( $R_n$ ). Averaged results for the execution of an MT with 4 (blue), 5 (ochre), 6 (green), 7 (red), and 8 (purple) leaf nodes.

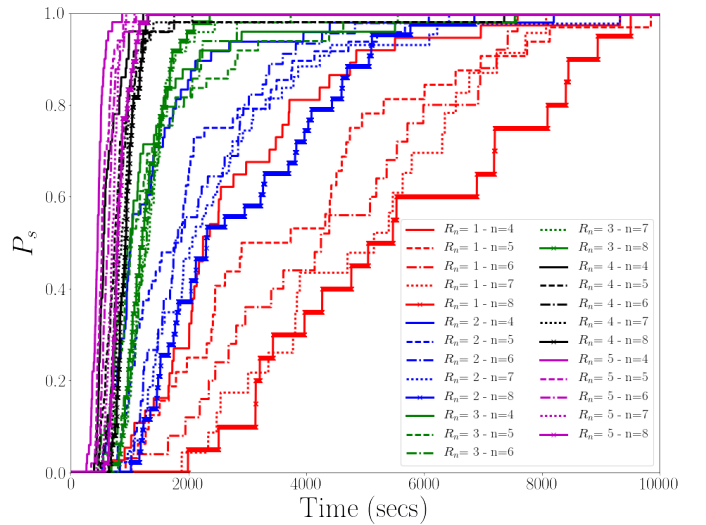


Figure 11. Probability of success ( $P_s$ ) for each one of the different configurations shown in Fig. 10. Empirical run-time distributions for the execution of the foraging task with  $R_n = 1$  (red), 2 (blue), 3 (green), 4 (black), and 5 (purple). For each one of these configurations solid ( $n = 4$ ), dashed ( $n = 5$ ), dot-dashed ( $n = 6$ ), dotted ( $n = 7$ ), and asterisk-solid ( $n = 8$ ) lines were included.

Fig. 11 shows the progression of  $P_s$  for all the configurations presented in Fig. 10. According to Fig. 11, the addition of more robots increases  $P_s$  since lines become steeper and converge to 1 (the maximum value) sooner. However, these results also suggest that as we increase  $n$  (the mission becomes longer),  $P_s$  converges to higher values later.

Fig. 12 shows averaged results and standard deviations for the Communication Cost (CC) in KB and Information Diversity (ID) as Shannon’s equitability index ( $I_e$ ) for different  $R_n \in (1 \leq R_n \leq 10)$  and  $n \in \{2,4,8\}$  configurations. Fig. 12 shows that CC increases linearly with  $R_n$  since there are more robots exchanging information. Moreover, MTs with larger  $n$  values also seem to increase the CC since the proofs robots exchange are “heavier”. Larger standard deviation values, as  $R_n$  increases, imply that there is no fixed number of P-V workflows required to make one robot complete its MT (finishing condition of the foraging mission). However, larger  $R_n$  values tend to increase the Information Diversity (ID) in the swarm. This result suggests that, as we increase  $R_n$ , the information

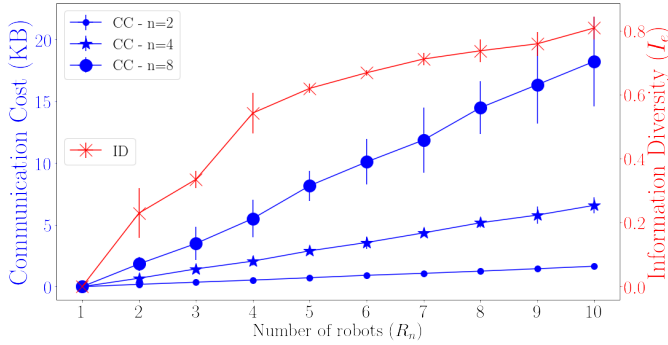
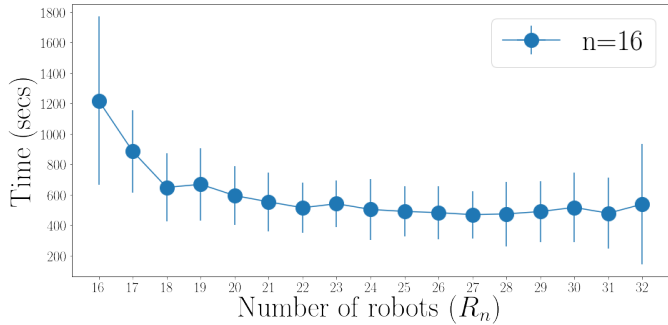
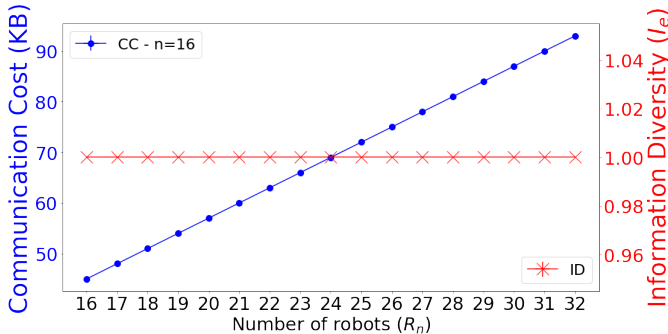


Figure 12. Communication Cost (CC) and Information Diversity (ID) metrics in blue and red colors, respectively, for different  $R_n$  and  $n$  values. Averaged results and standard deviations suggest a direct relationship between the two metrics in the foraging mission.

in the swarm tends to become more diversified. Fig. 12 also suggests that ID might have an asymptotic behavior around 0.8 and a really large  $R_n$  value might be necessary to converge to 1 (i.e., complete “evenness”).



(a) Average  $F_t$  (in secs) and standard deviations for the maze formation mission with different robot swarm sizes. All results represent a maze of an MT with 16 (blue) leaf nodes ( $n = 16$ ).



(b) Communication Cost (CC) and Information Diversity (ID) metrics in blue and red colors, respectively, for different  $R_n$  values for the maze formation mission. Averaged results and standard deviations suggest no direct relationship between the two metrics.

Figure 13. Different metrics for the maze formation mission. (a) shows the average  $F_t$  (in secs) and standard deviations while (b) shows Communication Cost (CC) in KB and Information Diversity (ID) as Shannon’s equitability index ( $I_e$ ).

To complement the results introduced previously, an additional set of 25 simulation experiments was carried out to analyze the maze formation mission (Fig. 9). In this case,  $n$  was fixed to 16 in order to match the number of cells where

the value 1 is present in Fig. 9 (a). In addition,  $R_n \in (n \leq R_n \leq 2n)$ . Fig. 13 (a) shows average  $F_t$  and standard deviations for the maze formation mission. Fig. 13 (a) shows the same behavior as its foraging counterpart (Fig. 10): larger  $R_n$  values reduce the  $F_t$ . However, beyond a certain  $R_n$  value ( $R_n \geq 20$ ), no real impact on the  $F_t$  can be seen. Complementarily, Fig. 13 (b) shows the CC and ID metrics for the maze formation mission. This figure also shows that CC increases linearly with  $R_n$ . However, in contrast to Fig. 12, the absence of increasing standard deviations confirms that a fixed CC is required to make all robots complete their MTs (finishing condition of the maze formation mission). Finally, Fig. 13 (b) depicts a scenario where complete “evenness” of information (i.e.,  $I_e = 1$ ) is achieved. This is possible since in the maze formation mission, when robots find a cell where they can generate a valid  $\pi$  proof, they stop at its center, thereby, making robots capable of fulfilling only one operation per mission, in contrast to the foraging scenario, where one robot might be able to complete several operations.

## V. DISCUSSION

In this research, we show how two of the main MT properties (i.e., correctness and security) open a new path towards secure and secret swarm robotic cooperation. Regarding the security aspect, by using the proposed approach, swarm robots are required to “prove” to their peers they fulfilled certain actions or they know or “own” particular information (i.e., proof-of-ownership [53]) to cooperate, rather than merely rely on information received from other robots (sensor data, votes, etc.). This approach makes robots resistant against potential threats such as tampering attacks since any alternation in the operation’s data (e.g.,  $h_i$ ,  $h_a$ ) will necessarily change the proof’s outcome. Regarding the secrecy component, with the use of MTs, swarm robots are now able to separate the mission data from its verification. This allows robots to verify that an operation was carried out by a member of the swarm in despite of not knowing what this operation entailed or what robot took part in its completion. This makes physical capture attacks inefficient since individual robots might not have enough raw or unprotected information to describe the high-level swarm’s missions and goals, especially, in large systems. However, this doesn’t prevent swarm robots from cooperating to fulfill complex missions since robots can still prove to their peers that certain operations were discovered, carried out, and completed.

The proposed approach was tested in two different scenarios: a foraging and a maze formation mission. In the foraging case, results suggest that  $R_n$  maintains an inverse relationship with  $F_t$  and a direct relationships with  $P_s$ . Therefore, increasing the swarm size has a positive impact on the performance of the system (i.e., the more the merrier). However, results also show that CC grows linearly as the swarm size ( $R_n$ ) increases, which in extreme situations (e.g., very large swarms) could represent a negative effect on the system since individual robots might not be able to cope with the bandwidth requirements. In contrast, increasing  $R_n$  has the positive effect of increasing the ID since we are increasing the probabilities of reaching more “even” distributions of completed operations within the swarm. Complementarily, we introduced the maze formation mission, where  $R_n$  and  $n$  take larger values. In the maze formation mission, results also suggest that  $R_n$  maintains an inverse relationship with  $F_t$ , ID is maximized (i.e., ID = 1),

and even though CC grows linearly, this still does not represent a challenging situation for the swarm (e.g., 90 KB for a 32 robot system). It is interesting to emphasize that due to these properties, swarm robots can fulfill complex missions such as the maze formation one without the means to infer high-level details such as where the entrance or the exit might be located.

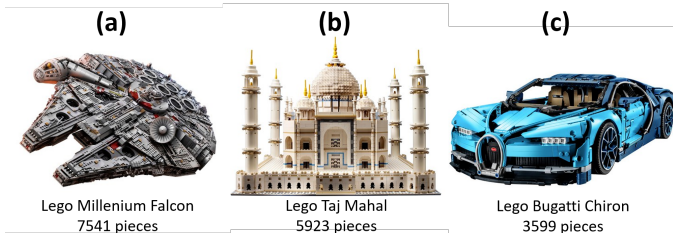


Figure 14. Different LEGO<sup>®</sup> models with their corresponding piece count. LEGO<sup>®</sup> models are a good projection of complex sequential missions that could be encapsulated in Merkle trees.

Fig. 14	Memory (KB)	CC/ $R_n$ (MB)	ACT (secs)
(a) Millennium Falcon (7541 pieces)	235 KB	3.39 MB	G: 8.45 (4.86) P: 0.0005 (1.54 e-5) V: 0.0006 (2.10 e-5)
(b) Taj Mahal (5923 pieces)	185 KB	2.54 MB	G: 6.62 (3.81) P: 0.0005 (1.87 e-5) V: 0.0006 (1.53 e-5)
(c) Bugatti Chiron (3599 pieces)	112 KB	1.46 MB	G: 4.01 (2.30) P: 0.0004 (1.58 e-5) V: 0.0005 (1.71 e-5)

TABLE I. Memory, Communication Cost per robot ( $CC/R_n$ ), and Average Computation Time (ACT) requirements (with standard deviations in brackets) for the models depicted in Fig. 14. All ACTs were obtained by using the Raspberry Pi 3 Model B+ SBC.

Encouraged by these results, we found appropriate to analyze the feasibility of the proposed approach in complex missions where the number of operations take relatively large values. Fig. 14 shows different LEGO<sup>®</sup> models where a sequential set of operations is required to achieve the final outcome (i.e., build the replica). These models<sup>3</sup> are good future projection of the missions presented in this work, especially, since  $n$  takes a relatively large value. Due to the possibility of accurately calculating the amount of CC required to make all robots complete their MTs (Eq. 1) as well as the overall size of the MT stored by robots ( $O(n)$ ), we can compute Fig. 14’s corresponding MTs and measure their memory, communication cost per robot ( $CC/R_n$ ) and Average Computation Time (ACT) requirements. For the latter, we included the following measures: generation of the complete Merkle tree (G), generation of a proof (P), and verification of a proof (V). Initial results for the aforementioned models are depicted in Table I.

Table I shows that neither the memory, communication cost per robot, nor the average computation time of the corresponding MTs is out of reach of the current commodity hardware (e.g., Raspberry Pi 3 Model B+) and therefore it is feasible for current robot platforms. It is important to note that more than 99% of the ACT is taken by the generation (G) of

the MT, while the proof assembly (P) and validation (V) take an almost insignificant amount of time. However, we would like to emphasize that the generation of the MT only takes place at the beginning of the mission and after completion, robots do not need to repeat it.

## VI. CONCLUSIONS

Swarm robotics is starting to show potential in both academic and real-world scenarios. However, achieving secure behaviors for large numbers of robots is still a challenging problem. Recent studies have emphasized the importance and lack of solutions for the security and privacy issues in the distributed robotics field. However, emerging lines of research such as the blockchain are starting to offer methods to address these problems. Merkle Trees (MTs) are binary hash-tree structures with two main properties: correctness and security. These properties have the potential to achieve secure and secret swarm robot cooperation and therefore make robotic swarms resistant against tampered members and physical capture attacks. By using MTs, swarm operators can provide the “blueprint” of the swarm’s objectives without disclosing raw or unprotected data about the mission itself. The performance, communication costs, and information diversity metrics of the proposed combination were analyzed for two different sequential missions: foraging (where robots modify the environment) and maze formation (where robots become the environment). Results show that larger numbers of robots tend to increase the performance of the system as well as diversify the amount of information within the swarm. However, an increasing number of robots as well as longer missions scale linearly together with the communication requirements of the system. Nevertheless, an initial analysis on the storage, communication costs, and computational time for higher-scale missions reveal that the use of MTs for current robotic technology is within reach. This study opens the door to design, test, and analyze complex robotic missions (e.g., with malicious actors) with this technique as well as implement the proposed approach with real-world hardware platforms.

## ACKNOWLEDGMENT

This project has received funding from the European Union’s Horizon 2020 research and innovation programme under the Marie Skłodowska-Curie grant agreement No. 751615.

## REFERENCES

- [1] R. D’Andrea, “Guest editorial: A revolution in the warehouse: A retrospective on Kiva Systems and the grand challenges ahead,” *IEEE Transactions on Automation Science and Engineering*, vol. 9, no. 4, 2012, pp. 638–639.
- [2] A. Bechar and C. Vigneault, “Agricultural robots for field operations. Part 2: Operations and systems,” *Biosystems Engineering*, vol. 153, jan 2017, pp. 110–128.
- [3] E. Castelló Ferrer, “The blockchain: A new framework for robotic swarm systems,” in *Proceedings of the Future Technologies Conference (FTC) 2018*, K. Arai, R. Bhatia, and S. Kapoor, Eds. Cham: Springer International Publishing, 2019, pp. 1037–1058.
- [4] F. Mondada et al., “The e-puck, a Robot Designed for Education in Engineering,” *Robotics*, vol. 1, no. 1, 2006, pp. 59–65.
- [5] E. Castello et al., “Adaptive foraging for simulated and real robotic swarms: the dynamical response threshold approach,” *Swarm Intelligence*, vol. 10, no. 1, 2016, pp. 1–31.

<sup>3</sup>Three of the replicas with the largest piece count according to the current LEGO<sup>®</sup> catalog: <https://shop.lego.com/en-US/>

- [6] D. Chaudhari and S. A. Bhosale, "A review on management of logistics using swarm robotics," in 2016 International Conference on Communication and Signal Processing (ICCCSP). IEEE, apr 2016, pp. 0371–0373.
- [7] A. L. Alfeo et al., "Urban swarms: A new approach for autonomous waste management," *CoRR*, vol. abs/1810.07910, 2018.
- [8] G.-Z. Yang et al., "The grand challenges of science robotics," *Science Robotics*, vol. 3, no. 14, 2018.
- [9] S. Paul, "Robotics on the Battlefield Part II: The Coming Swarm," Center for New American Security, Tech. Rep., 10 2014.
- [10] R. N. Akram et al., "Security, Privacy and Safety Evaluation of Dynamic and Static Fleets of Drones," 2017.
- [11] S. Gil, S. Kumar, M. Mazumder, D. Katabi, and D. Rus, "Guaranteeing spoof-resilient multi-robot networks," *Autonomous Robots*, vol. 41, no. 6, Aug 2017, pp. 1383–1400.
- [12] A. Prorok and V. Kumar, "A macroscopic privacy model for heterogeneous robot swarms," in *Lecture Notes in Computer Science (including subseries Lecture Notes in Artificial Intelligence and Lecture Notes in Bioinformatics)*, ser. *Lecture Notes in Computer Science*, M. Dorigo et al., Eds. Springer International Publishing, 2016, vol. 9882 LNCS, pp. 15–27.
- [13] A. Prorok and V. K., "Towards differentially private aggregation of heterogeneous robots," in *Distributed Autonomous Robotic Systems: The 13th International Symposium*. Springer International Publishing, 2018, pp. 587–601.
- [14] A. G. Millard, J. Timmis, and A. F. T. Winfield, "Towards Exogenous Fault Detection in Swarm Robotic Systems," 2014, pp. 429–430.
- [15] J. D. Bjercknes and A. F. T. Winfield, "On Fault Tolerance and Scalability of Swarm Robotic Systems," in *Springer Tracts in Advanced Robotics*, 2013, vol. 83 STAR, pp. 431–444.
- [16] F. Higgins, A. Tomlinson, and K. M. Martin, "Survey on Security Challenges for Swarm Robotics," in 2009 Fifth International Conference on Autonomic and Autonomous Systems. IEEE, 2009, pp. 307–312.
- [17] A. F. Winfield and J. Nembrini, "Safety in numbers: fault-tolerance in robot swarms," *International Journal of Modelling, Identification and Control*, vol. 1, no. 1, 2006, p. 30.
- [18] I. Sargeant and A. Tomlinson, "Review of Potential Attacks on Robotic Swarms," in *Proceedings of SAI Intelligent Systems Conference (IntelliSys) 2016*, ser. *Lecture Notes in Networks and Systems*, Y. Bi, S. Kapoor, and R. Bhatia, Eds., vol. 15. Cham: Springer International Publishing, 2016, pp. 628–646.
- [19] V. Strobel, E. Castelló Ferrer, and M. Dorigo, "Managing byzantine robots via blockchain technology in a swarm robotics collective decision making scenario," in *Proceedings of the 17th International Conference on Autonomous Agents and MultiAgent Systems*, ser. *AAMAS '18*. Richland, SC: International Foundation for Autonomous Agents and Multiagent Systems, 2018, pp. 541–549.
- [20] L. Parker, "Distributed Intelligence: Overview of the Field and its Application in Multi-Robot Systems," *Journal of Physical Agents*, vol. 2, no. 1, 2008, pp. 5–14.
- [21] C. R. Kube and H. Zhang, "Collective robotics: From social insects to robots," *Adapt Behav*, vol. 2, no. 2, Sep. 1993, pp. 189–218.
- [22] E. Bonabeau, M. Dorigo, and G. Theraulaz, "Inspiration for optimization from social insect behavior," *Nature*, vol. 406, 08 2000, pp. 39–42.
- [23] M. Duarte et al., "Evolution of collective behaviors for a real swarm of aquatic surface robots," *PLOS ONE*, vol. 11, no. 3, 03 2016, pp. 1–25.
- [24] M. Rubenstein, A. Cornejo, and R. Nagpal, "Programmable self-assembly in a thousand-robot swarm," *Science*, vol. 345, no. 6198, 2014, pp. 795–799.
- [25] F. Ducatelle et al., "Cooperative navigation in robotic swarms," *Swarm Intelligence*, vol. 8, no. 1, Mar 2014, pp. 1–33.
- [26] M. Rubenstein, C. Ahler, N. Hoff, A. Cabrera, and R. Nagpal, "Kilobot: A low cost robot with scalable operations designed for collective behaviors," *Robotics and Autonomous Systems*, vol. 62, no. 7, 2014, pp. 966 – 975, reconfigurable Modular Robotics.
- [27] F. Mondada et al., "The e-puck, a robot designed for education in engineering," in *In Proceedings of the 9th Conference on Autonomous Robot Systems and Competitions*, 2009, pp. 59–65.
- [28] O. Holland and C. Melhuish, "Stigmergy, self-organization, and sorting in collective robotics," *Artificial Life*, vol. 5, no. 2, 1999, pp. 173–202.
- [29] O. Zedadra, H. Seridi, N. Jouandeau, and G. Fortino, "Design and analysis of cooperative and non cooperative stigmergy-based models for foraging," in *Computer Supported Cooperative Work in Design (CSCWD)*, 2015 IEEE 19th International Conference on. IEEE, 2015, pp. 85–90.
- [30] A. A. Khalik, "From ants to service robots : an exploration in stigmergy-based navigation algorithms," Ph.D. dissertation, Örebro University, School of Science and Technology, 2018.
- [31] A. L. Alfeo, M. G. C. A. Cimino, N. De Francesco, A. Lazzeri, M. Lega, and G. Vaglini, "Swarm coordination of mini-uavs for target search using imperfect sensors," *Intelligent Decision Technologies*, no. 12, 2018, pp. 149–162.
- [32] J. Werfel, K. Petersen, and R. Nagpal, "Designing collective behavior in a termite-inspired robot construction team," *Science*, vol. 343, no. 6172, 2014, pp. 754–758.
- [33] R. Grabowski, L. E. Navarro-Serment, C. J. Paredis, and P. K. Khosla, "Heterogeneous teams of modular robots for mapping and exploration," *Autonomous Robots*, vol. 8, no. 3, Jun 2000, pp. 293–308.
- [34] N. Michael et al., "Collaborative mapping of an earthquake-damaged building via ground and aerial robots," *Journal of Field Robotics*, vol. 29, no. 5, 2012, pp. 832–841.
- [35] W. Burgard, M. Moors, and F. Schneider, "Collaborative exploration of unknown environments with teams of mobile robots," in *Advances in Plan-Based Control of Robotic Agents*, M. Beetz, J. Hertzberg, M. Ghallab, and M. E. Pollack, Eds. Berlin, Heidelberg: Springer Berlin Heidelberg, 2002, pp. 52–70.
- [36] Z. Beck, L. Teacy, A. Rogers, and N. R. Jennings, "Online planning for collaborative search and rescue by heterogeneous robot teams," in *Proceedings of the 2016 International Conference on Autonomous Agents and Multiagent Systems*, ser. *AAMAS '16*. Richland, SC: International Foundation for Autonomous Agents and Multiagent Systems, 2016, pp. 1024–1033.
- [37] N. Michael, J. Fink, and V. Kumar, "Cooperative manipulation and transportation with aerial robots," *Autonomous Robots*, vol. 30, no. 1, 2011, pp. 73–86, cited By 281.
- [38] D. Mellinger, M. Shomin, N. Michael, and V. Kumar, "Cooperative grasping and transport using multiple quadrotors," *Springer Tracts in Advanced Robotics*, vol. 83 STAR, 2012, pp. 545–558, cited By 151.
- [39] M. Dunbabin and L. Marques, "Robots for environmental monitoring: Significant advancements and applications," *IEEE Robotics and Automation Magazine*, vol. 19, no. 1, 2012, pp. 24–39, cited By 133.
- [40] A. Flores-Abad, O. Ma, K. Pham, and S. Ulrich, "A review of space robotics technologies for on-orbit servicing," *Progress in Aerospace Sciences*, vol. 68, 2014, pp. 1–26, cited By 334.
- [41] R. C. Merkle, "A Digital Signature Based on a Conventional Encryption Function," 1988, pp. 369–378.
- [42] F. Li, M. Hadjieleftheriou, G. Kollios, and L. Reyzin, "Dynamic authenticated index structures for outsourced databases," in *Proceedings of the 2006 ACM SIGMOD International Conference on Management of Data*, ser. *SIGMOD '06*. New York, NY, USA: ACM, 2006, pp. 121–132.
- [43] D. Hintze and A. Rice, "Picky: Efficient and reproducible sharing of large datasets using merkle-trees," *Proceedings - 2016 IEEE 24th International Symposium on Modeling, Analysis and Simulation of Computer and Telecommunication Systems, MASCOTS 2016*, 2016, pp. 30–38.
- [44] M. S. Niaz and G. Saake, "Merkle hash tree based techniques for data integrity of outsourced data," *CEUR Workshop Proceedings*, vol. 1366, 2015, pp. 66–71.
- [45] W. Du, R. Wang, and P. Ning, "An efficient scheme for authenticating public keys in sensor networks," in *Proceedings of the 6th ACM International Symposium on Mobile Ad Hoc Networking and Computing*, ser. *MobiHoc '05*. New York, NY, USA: ACM, 2005, pp. 58–67.
- [46] L. Zhou and C. Ravishankar, "Dynamic Merkle Trees for Verifying Privileges in Sensor Networks," in 2006 IEEE International Conference on Communications, vol. 5, no. c. IEEE, 2006, pp. 2276–2282.
- [47] H. Halpin, "Updatechain: Using Merkle Trees for Software Updates," 2016, pp. 1–15.

- [48] B. P. Gerkey and M. J. Matarić, "A Formal Analysis and Taxonomy of Task Allocation in Multi-Robot Systems," *The International Journal of Robotics Research*, vol. 23, no. 9, sep 2004, pp. 939–954.
- [49] M. Dorigo et al., "Swarmanoid: A novel concept for the study of heterogeneous robotic swarms," *IEEE Robotics Automation Magazine*, vol. 20, no. 4, Dec 2013, pp. 60–71.
- [50] C. Pinciroli et al., "ARGoS: a modular, parallel, multi-engine simulator for multi-robot systems," *Swarm Intelligence*, vol. 6, no. 4, dec 2012, pp. 271–295.
- [51] L. Garattoni and M. Birattari, "Autonomous task sequencing in a robot swarm," *Science Robotics*, vol. 3, no. 20, jul 2018.
- [52] C. E. Shannon, "A mathematical theory of communication," *Bell System Technical Journal*, vol. 27, no. 3, 1948, pp. 379–423.
- [53] S. Halevi, D. Harnik, B. Pinkas, and A. Shulman-Peleg, "Proofs of ownership in remote storage systems," in *Proceedings of the 18th ACM Conference on Computer and Communications Security*, ser. CCS '11. New York, NY, USA: ACM, 2011, pp. 491–500.